

Congenital and Acquired Atrophy of the Shoulder Girdle Muscles in a Patient with Sprengel's Deformity

James D. Collins, MD

Keywords: Sprengel's deformity ■ omovertebra ■ magnetic resonance imaging ■ magnetic resonance angiography ■ magnetic resonance venography ■ radiology ■ anatomy ■ costoclavicular compression

J Natl Med Assoc. 2011;103:635-643

Author Affiliations: University of California at Los Angeles, Department of Radiological Sciences, Los Angeles, California.

Correspondence: James D. Collins, MD, University of California at Los Angeles, Department of Radiological Sciences, 10833 Le Conte Ave, BL-428 CHS/UCLA mail code 172115, Los Angeles, CA 90095 (jamesc@mednet.ucla.edu).

INTRODUCTION

Sprengel's deformity is a congenital anomaly of the shoulder girdle which results in elevation of the scapula (congenital high scapula) and limitation of movement of the shoulder.¹ Sprengel's deformity is the most common congenital malformation of the shoulder girdle, with a male to female ratio of 3:1. It is frequently associated with cervical spine malformations, absent or hypoplastic periscapular musculature, and abnormalities in the cervicothoracic vertebrae or thoracic rib cage: absent or fused ribs, chest wall asymmetry, Klippel-Feil syndrome, cervical ribs, congenital scoliosis, and cervical spina bifida.

The hallmark of Sprengel's deformity is shoulder asymmetry with restriction of shoulder abduction. The elevation of the scapula is accompanied by its rotation to various positions. Clinically, the affected scapula is usually elevated 2 to 10 cm, adducted, and its inferior pole is medially rotated. The left side is more commonly affected but may sometimes be bilateral, in which case it is more functionally disabling, although it is cosmetically much more acceptable.

No satisfactory explanation exists regarding the pathogenesis of Sprengel's deformity. It is thought to be the consequence of teratogenic exogenous or endogenous harmful agent affecting mesenchymal tissue in the fourth to fifth week of embryogenesis. There may be hereditary forms. There is underdevelopment and

degeneration of the shoulder girdle muscles and creation of abnormal omovertebral fibrous, cartilaginous or osseous connection, such as the presence of an omovertebral bone seen in approximately one-third of patients. The hypoplastic scapula is usually tethered to the spine and posterior ribs by tight bands or by the omovertebral bone, which restricts scapular movements, and therefore abduction of the arm. The diagnosis of Sprengel's deformity is based on clinical examination and radiological findings.

It is uncommon to identify an adult with untreated Sprengel's deformity, like the patient who presented here. Most patients with Sprengel's deformity receive surgical treatment as children or adolescents.

Adult patients with childhood polio, an acquired cause of weakness of the shoulder girdle, may present later in life with symptoms and signs of thoracic outlet syndrome with worsening of the weakness.²⁻⁴ The accompanying pain and sensory symptoms such as tingling and "numbness" would mitigate against a diagnosis of post polio syndrome in these patients.

CLINICAL HISTORY

The patient was a very pleasant 39-year-old, left-handed woman who presented for evaluation of thoracic outlet syndrome. The patient was diagnosed as an infant with Sprengel's deformity, atrophy of her left shoulder, arm, and hand musculature. The presenting symptoms were referable to the left side. The right side was asymptomatic. Her current symptoms included atrophy, pain, numbness, tingling, and weakness of the left shoulder and hand. Using a 10-point somatic pain scale, her pain at the time was scored at 8. Initially, she was diagnosed with carpal tunnel syndrome and underwent decompression surgery. However, her symptoms progressed to include difficulty driving, brushing her teeth, combing her hair, carrying objects, lifting her child with her left arm, and loss of left hand function. She was evaluated by a neurologist, who referred her to another neurologist, who then suggested she had clinical diagnosis of thoracic outlet syndrome and that she needed to define the anatomy of her left shoulder deformity—Sprengel's deformity. Bilateral magnetic resonance imaging (MRI), magnetic

resonance angiography (MRA), and magnetic resonance venography (MRV) of the brachial plexus were requested to determine sites of brachial compression.⁵

PHYSICAL EXAMINATION

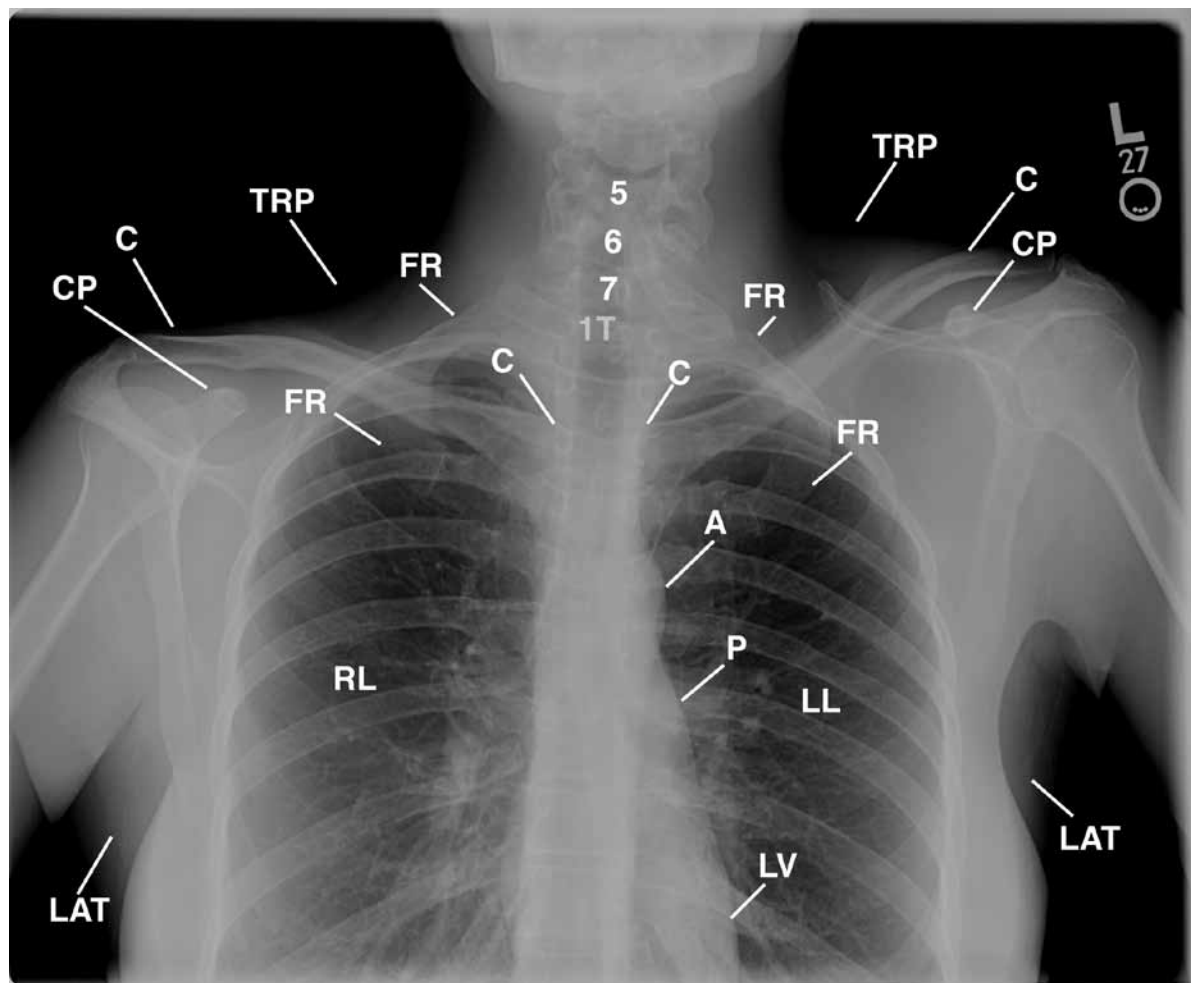
Blood pressure in the right arm was 121/82 mm Hg; pulse, 70 beats/min; respiration, 17 breaths/min; temperature, 97.9°F. She was positive for the forward-elevated left shoulder “hump”—otherwise unremarkable. The patient added that she had experienced floaters without blurred vision, back pain down to the waist, and experienced unconsciousness one time.

MATERIALS AND METHODS

Plain chest radiographs (posterior-anterior and lateral) were obtained and reviewed prior to the MRI. The

procedure was discussed and the patient examined. Respiratory gating was applied throughout the procedure to minimize motion artifact. The patient was supine in the body coil, arms down to the side, and imaging was monitored at the MRI station. Magnetic resonance images were obtained on the 1.5 Tesla GE Signa MR scanner (GE Medical Systems, Milwaukee, Wisconsin). A body coil was used, and intravenous contrast agents were not administered. A water bag was placed on the right and the left side of the neck to increase the signal to noise ratio for high-resolution imaging. A full field of view (44 cm) of the neck and the thorax was used to image the supraclavicular fossae. Contiguous (4 mm) coronal, transverse (axial), oblique transverse, sagittal, abduction external rotation (AER, of the upper extremities) T1-weighted images, and 2-dimensional

Figure 1. Posterior-Anterior Chest Radiograph



Head leaning right, accentuating the left concave scoliosis of the cervicothoracic spine, C4-T5; left concave “spade-like ossification” (omovertebral bar or bone) extending from the spinous process of C6 over the left cervical rib that does not unite with the first rib and/or the left scapula; elevated left shoulder, and increased lucency of the left neck and shoulder compared to the right, reflecting atrophy of the left trapezius muscle compared to the right.

A, aorta; C, clavicle; CP, coracoid process; FR, first rib; LAT, latissimus dorsi muscle; LL, left lung; LV, left ventricle; P, pulmonary artery; T, trachea; TRP, trapezius muscle; 1T, first thoracic vertebra; 5,6,7, fifth, sixth, seventh cervical vertebrae.

time-of-flight MRA were obtained. If there was clinical evidence of scarring, tumor and/or lymphatic obstruction, fast-spin echo T2-weighted images would have been selectively obtained. The parameters for acquiring each sequence have been published.

POSTERIOR-ANTERIOR AND LATERAL CHEST RADIOGRAPHIC FINDINGS

No previous chest films were present for comparison. The posterior-anterior chest radiograph (Figure 1) displays the head leaning right, accentuating the left concave scoliosis of the cervicothoracic spine, C4-T5; left concave “spade-like ossification” (omovertebral bar or bone), extending from the spinous process of C6 over the left cervical rib that does not unite with the first rib and/or the left scapula; drooping right shoulder as compared to the anterior-rotated elevated left shoulder; narrowed left interscostal spaces posteriorly reflecting the mild concave scoliosis as above described; increased lucency of the left neck and shoulder as compared to the right, reflecting atrophy of the left trapezius muscle as

compared to the right; anterior-rotated heads of the clavicles over the posterior third interscostal space, accentuating the sloping of the left first rib as compared to the right first rib; possible fusion of the lateral masses of the cervical spine from C5-C6 superiorly; and narrowed cardiomeastinal structures and normal lungs.

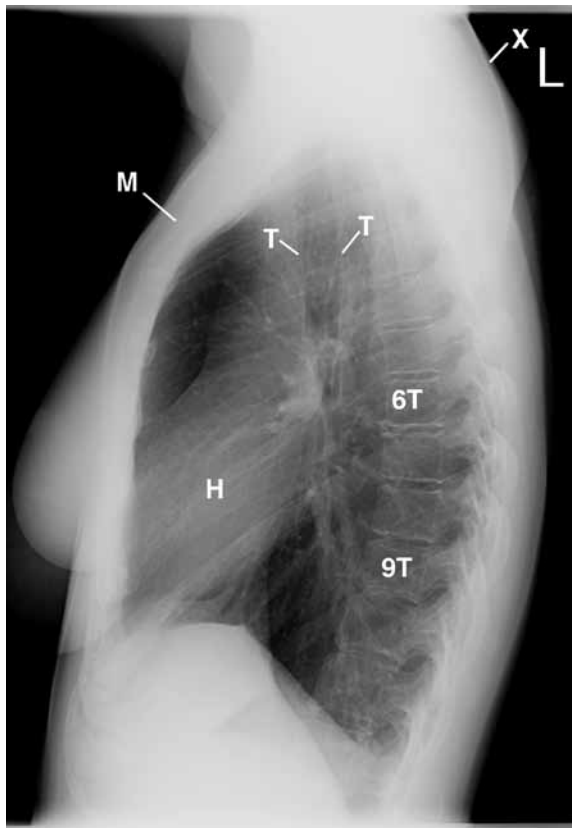
The lateral chest radiograph (Figure 2) displays elevation of the left shoulder, reflecting the slight wing-like appearance of the scapula; mild kyphosis of the thoracic spine, accentuated by the anterior bowed body of the sternum and the backward displaced manubrium; foreshortened left breast superimposed on the lower right breast; and normal cardiomeastinal structures and lungs.

The anterior-posterior cervicothoracic spine radiograph (Figure 3) displays the incomplete separation of the lateral pillars bilaterally and superior to the C6 vertebra, and the small cervical ribs, left greater than right.

CHEST RADIOGRAPHS CONCLUSION(S)

- Sprengel’s deformity, left shoulder.
- Omovertebral ossification as above, extending from the left C6 spinous process laterally to the scapula.
- Left concave scoliosis cervicothoracic spine, C4-T5.
- Question of fused lateral pillars of the cervical spine as above.
- Atrophy of the left sling/erector muscles.

Figure 2. Lateral Chest Radiograph



Elevation of the left shoulder backward displacement of the manubrium sterni (M); mild kyphosis of the cervicothoracic spine accentuated by the anterior bowed body of the sternum; foreshortened left breast superimposed on the lower right breast, and rounding of the shoulders (X).

H, heart; T, trachea; X, rounding of the shoulders; 6T, 9T, sixth and ninth thoracic vertebrae.

Figure 3. Cervicothoracic Spine Radiograph



Incomplete separation of the lateral pillars bilaterally and superior to the C6 vertebra, and the small cervical ribs (CR), left greater than right. Observe the omovertebral bone (small arrows).

C, clavicle; FR, first rib; RL, right lung, T, trachea; 1T, first thoracic vertebra; 5, fifth cervical vertebra.

- Post-carpal tunnel release left wrist.
- Small cervical ribs, left greater than right.

TECHNIQUE

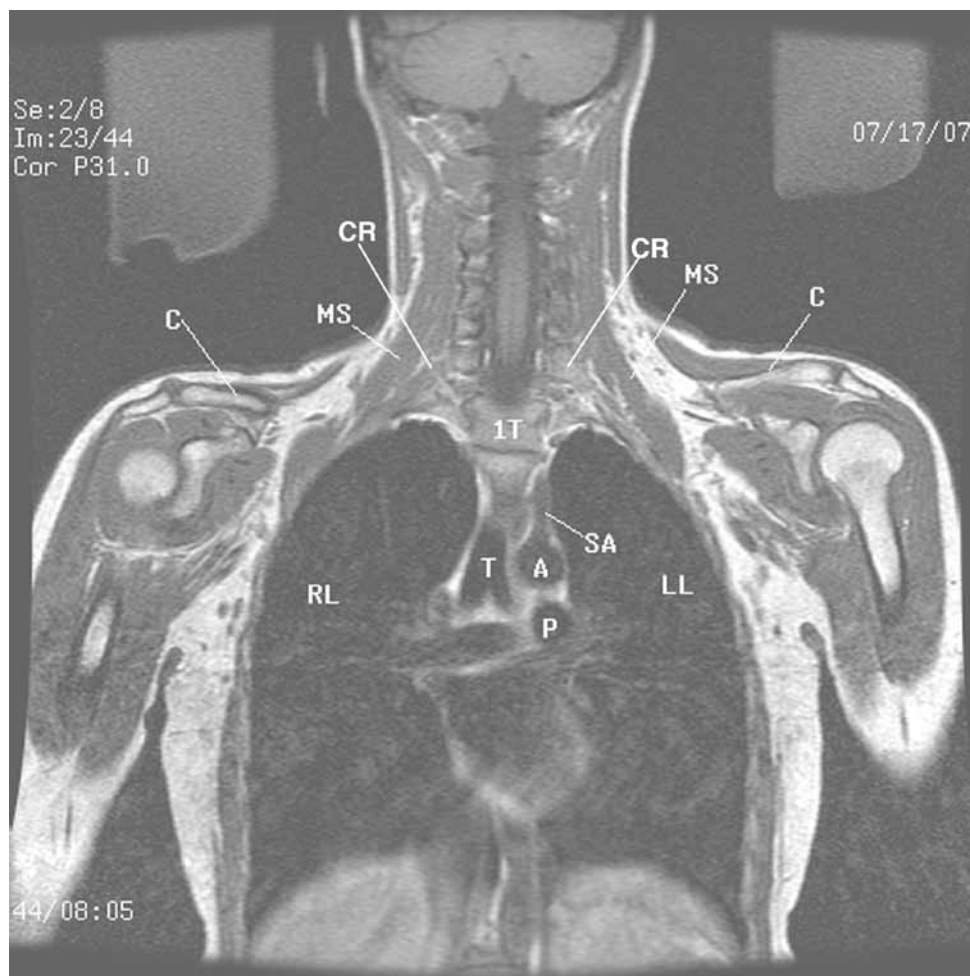
Bilateral MRI/MRA/MRV of the brachial plexus were conducted on the 1.5 Tesla LX Signa Unit, 9.0 software, 512 × 256 matrix, 44 × 44 cm field of view, saline water bags alongside the neck to enhance signal to noise ratio, 4-mm thickness. Coronal, transverse, transverse oblique, sagittal, bilateral coronal AER of the upper extremities 2-dimensional time-of-flight MRA/MRV sequences were obtained. Selected reformat 3-dimensional reconstruction of the coronal, transverse, and sagittal sequences was also evaluated. Selected enlarged images were annotated for physician's preview.

MULTIPLANAR MAGNETIC RESONANCE IMAGING FINDINGS

Multiplanar MRI cross-referenced the chest radiographs to display cervical ribs (Figure 4); atrophic left trapezius and rhomboid muscles (Figures 5 and 6); omovertebra extending from the medial margin of the left scapula to the sixth cervical vertebra (Figure 7); rotated head and neck right secondary to the omovertebral osseous abnormality and pain on the left as compared to the right throughout all series acquired. Atrophy of the left anterior scalene, middle, and posterior scalene muscles with the elevated scapula was observed on the left as compared to the right.

The posterior sloping right of the manubrium placed the head of the right clavicle posterior to the left. The thymus gland (Figure 7) was observed as above described with the rotated dominant shoulder as compared to the left. The clavicles and subclavius muscles compressed

Figure 4. Coronal T1-Weighted Magnetic Resonance Imaging Sequence



Head and neck leaning right, accentuating mild right concave scoliosis of the cervicothoracic spine, C2-T6; elevated left shoulder; increased soft tissue fat over the left posterior neck, accentuating the atrophy of the trapezius muscle; atrophy of the left middle scalene (MS) muscles compared to the right
 A, aorta; C, clavicle; CR, cervical ribs; LL, left lung; P, pulmonary artery; RL, right lung; SA, subclavian artery; T, trachea; 1T, first thoracic vertebra.

the subclavian veins, greater left than right, with collateral venous return from the right vertebral vein and the external jugular vein as compared to decreased venous return from the left external jugular vein compressed on the bicuspid valve of the left subclavian vein.

Atrophy of the left trapezius and the rhomboid major muscles were displayed greater left than right. The clavicles with the subclavius muscles compressed the subclavian veins as above described with compression of the subclavian arteries with binding nerve roots. However, the left head of the clavicle was rotated posteriorly as compared to the near vertical head of the right clavicle.

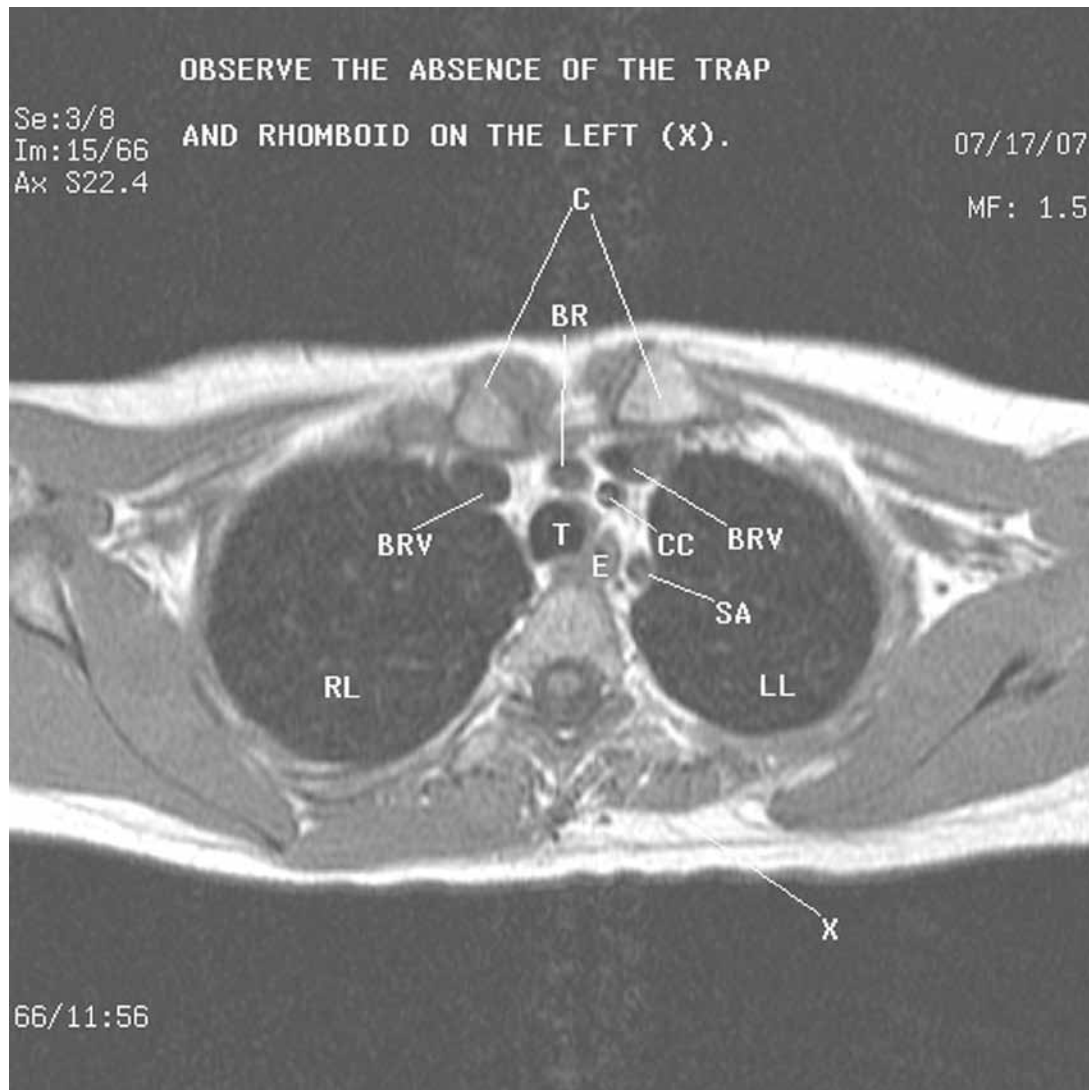
Low signal intensity of the left axillary vein suggested greater venous return than on the left. However,

the subclavian vein on the right was compressed greater than the left. The incomplete descent of the left shoulder elevated as above described reflected the Sprengel's deformity as above described without definitive fusion to the left scapula.

Two-dimensional time-of-flight MRA and MRV (Figure 8) cross-referenced the chest and T1-weighted images to display greater impedance to venous and arterial flow on the left as compared to the right.⁶ In fact, the right vertebral vein and the external jugular vein provided greater collateral circulation than on the left as above described.

Bilateral AER of the upper extremities triggered an uncomfortable sensation on the right and left arms and

Figure 5. Transverse Magnetic Resonance Imaging Sequence



Forward-rotated dominant right shoulder compared to the left, small left hemithorax compared to the right, manubrium sloping posterior and to the right placing the head of the right clavicle (C) posterior to the left, marked atrophy of the left rhomboid major and trapezius muscles replaced by high signal intensity fat (X).

BR, brachiocephalic artery; BRV, brachiocephalic vein; CC, common carotid artery; E, esophagus; LL, left lung; RL, right lung; SA, subclavian artery; T, trachea.

hands, with numbness before the procedure began and stayed numb on completion of the procedure. Gray floaters were visualized. I injected 10 mg of Valium (3-mg increment dosages) for conscious sedation, which may have had some diminishing responses.

MRI CONCLUSIONS

- Thin subcutaneous tissues and narrow thorax.
- Sprengel's deformity as described above without communication with the medial margin of the left scapula.
- Omovertebral bone and/or bar structure as above described into the left neck and soft tissues.
- Atrophy of the left trapezius, rhomboid, and the levator scapulae muscles as well as the serratus anterior muscle on the left as compared to the right.
- Asymmetric breast secondary to the deformity as above described.
- Left concave kyphoscoliosis of the thoracic spine.
- Bilateral costoclavicular compression (laxity of the sling/erector muscles—trapezius, levator scapulae, and serratus anterior muscles) of the

bicuspid valves within the draining veins of the neck, supraclavicular fossae with the subclavian and axillary arteries and binding nerve roots, right greater than left.

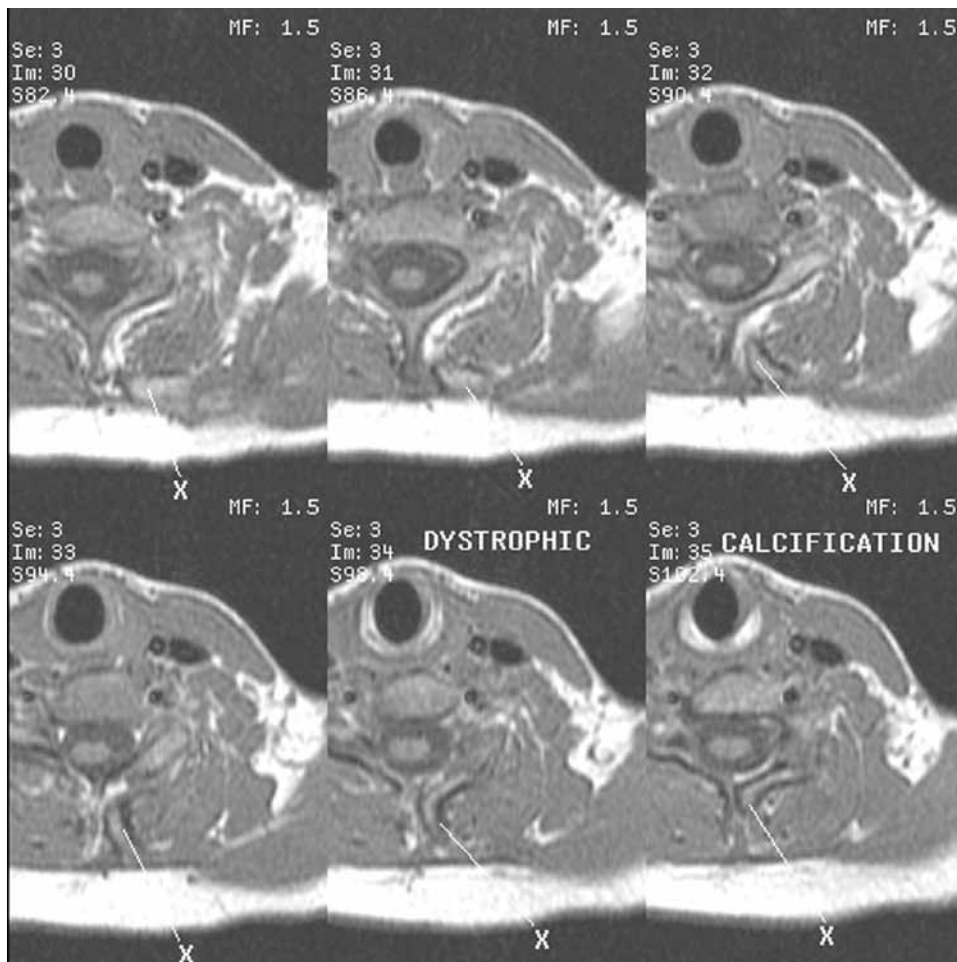
- Possible right interscalene triangle fibrosis.
- Bilateral AER of the upper extremities triggered an uncomfortable sensation on the right—and what the patient describes as numbness on the left—that is always there and not changed. The patient described gray-like visual floaters and no headaches. The patient required 10 mg of Valium for conscious sedation.

DISCUSSION

Associated malformations are almost always present with a Sprengel deformity. These can include anomalies in the cervicothoracic vertebrae or the thoracic rib cage. When scoliosis is present, the most common curves are in the cervicothoracic or upper thoracic region. A relationship between a Sprengel deformity and diastematomyelia has also been shown.

Another anomaly is the omovertebral bone. This is a

Figure 6. Serial Transverse Sequence of Dystrophic Omovertebra (X) Images 30 to 35



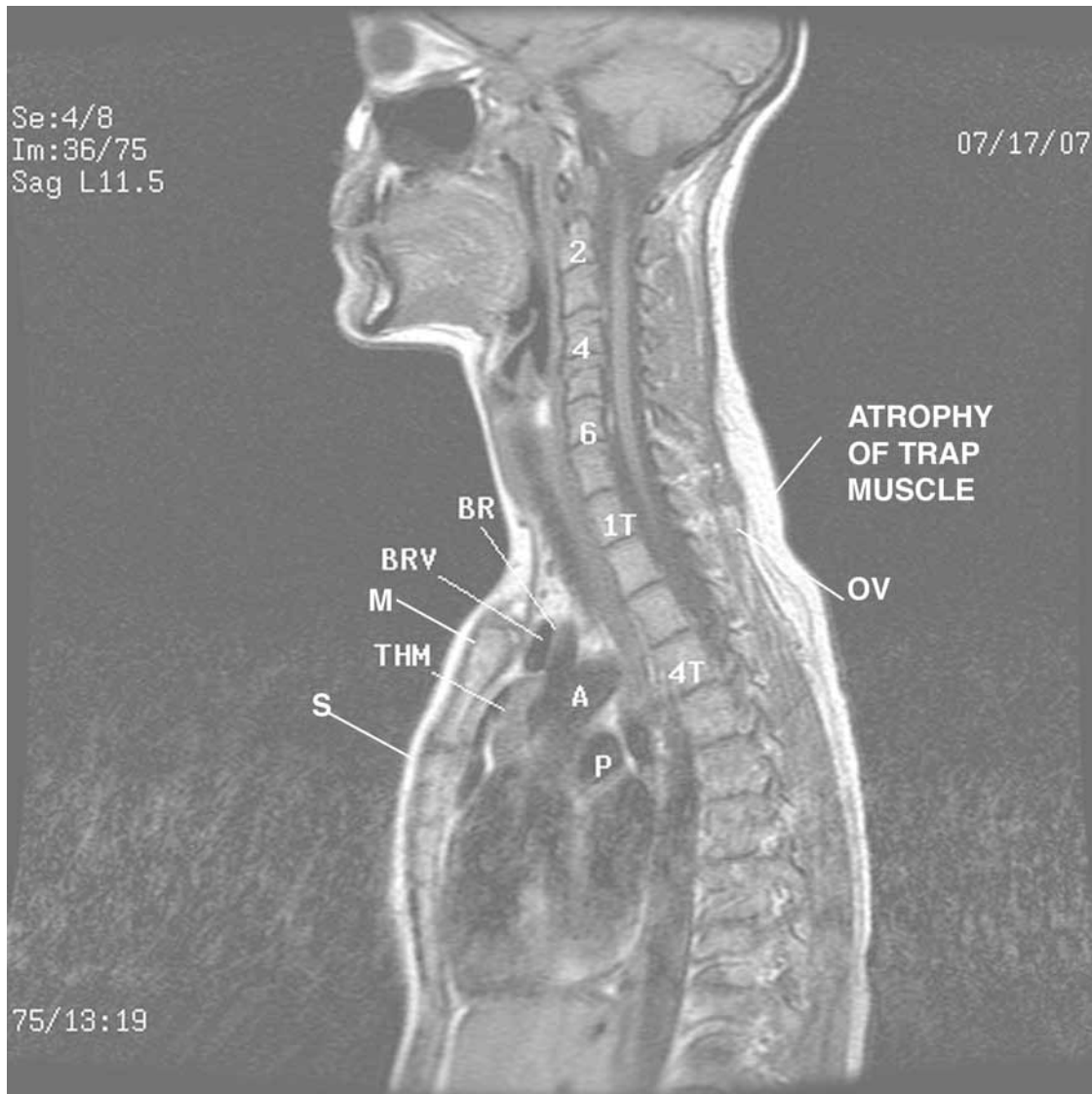
rhomboid- or trapezoid-shaped structure of cartilage or bone that usually lies in a strong fascial sheath, which extends from the superomedial border of the scapula to the spinous processes, lamina, or transverse processes of the cervical spine—most commonly the fourth to seventh cervical vertebrae. A well-developed joint can form between the scapula and the omovertebral bone; this bone can also be a solid osseous bridge. The omovertebral bone is best visualized on a lateral or oblique radiograph of the cervical spine.

Due to this rotation, the glenoid faces inferiorly. A prominence in the suprascapular region is characteristic due to the upwardly rotated superomedial angle of the

scapula, which causes the ipsilateral side of the neck to appear fuller and its normal contour to be lost. The scapula is hypoplastic, and the length of the vertebral border is decreased. Occasionally, some anterior bending of the supraspinous portion is present.

Passive movement of the glenohumeral joint, including abduction and external and internal rotation, may be normal. However, scapulothoracic movements may be severely limited. In 40% of patients with a Sprengel deformity, combined abduction is limited to less than 100°. The omovertebral bone may also limit abduction by affecting scapular mobility and can also limit neck movement if this bone is attached high in the cervical

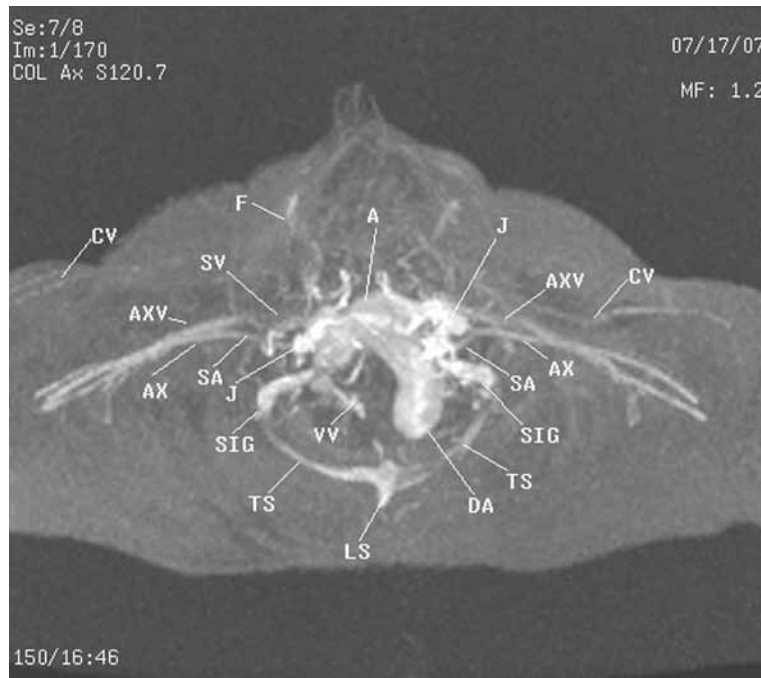
Figure 7. Midsagittal Image



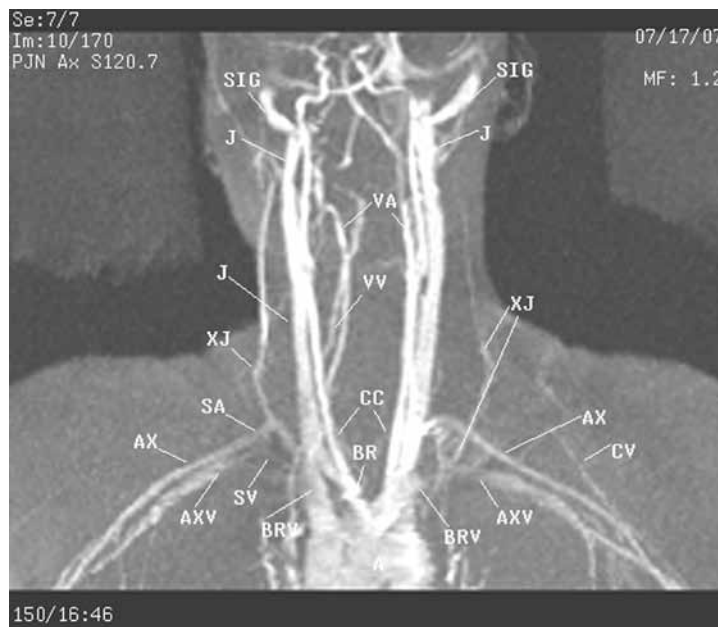
Gray proton density of the thymus gland (THM) within the capsule posterior to the manubrium and slightly extending up to the margins of the brachiocephalic vein (BRV), backward-displaced manubrium, accentuating the very mild anterior bowing of the sternum (S) and kyphosis of the thoracic spine (C6-4T).

A, aorta; BR, brachiocephalic artery; P, pulmonary artery; 2,4,6, second, fourth, and sixth cervical vertebrae; 1T, 4T, first and fourth thoracic vertebrae.

FIGURE 8A. Magnetic Resonance Angiography and Magnetic Resonance Venography



Two-dimensional time-of-flight magnetic resonance angiography and magnetic resonance venography stacked image displays the dominant forward right shoulder; longitudinal sinus (LS) draining into the dominant right transverse (TS) into the sigmoid sinus (SIG) compared to the smaller left transverse sinus; backward-displaced mildly compressed left subclavian artery (SA) and proximal dilatation of the axillary vein (AXV), reflecting greater impedance to venous return on the left; small left cephalic vein (CV) providing collateral circulation to the dilated left axillary vein; near-parallel rotation of the right axillary artery (AX) and vein (AXV), reflecting the greater forward rotation of the right hemithorax compared to the left; dominant left internal jugular vein (J) compared to the right.



Two-dimensional time-of-flight coronal 3-dimensional reconstructed magnetic resonance angiography and magnetic resonance venography displays the head and neck leaning right; increased signal intensity of the small right external jugular vein (XJ) compared to the very faint gray proton density of the left external jugular vein; mild compression of the second division of the right subclavian artery (SA) with proximal dilatation as it courses posterior to the narrowed bicuspid valve region of the right internal jugular vein (J); compression of the diminished signal intensity right subclavian vein (SV). Observe the collateral circulation provided by the right vertebral vein (VV) reflecting the collateral increase in venous return on the right vertebral compared to the left.

A; aorta; AX, axillary artery; AXV, axillary vein; BR, brachiocephalic artery; BRV, brachiocephalic vein; CC, common carotid artery; CV, cephalic vein; DA, descending aorta; F, facial vein; J, jugular vein; LS, longitudinal sinus; SA, subclavian artery; SIG, sigmoid sinus; SS, straight sinus; SV, subclavian vein; TS, transverse sinus; VA, vertebral artery; VV, vertebral vein; XJ, external jugular vein.

spine. Other causes of limited abduction include abnormal and weakened scapular muscles.

With her skeletal anomalies, it would appear that her brachial plexus and subclavian artery were being displaced. This in turn resulted in loss of nerve function to her left arm and hand. Clinically, this appeared in the form of muscle atrophy and loss of strength and function in her left arm and hand. Based on this, there were several reasons to proceed with surgery: to alleviate the compression of her nerve and prevent further loss of muscle and strength, to allow what nerve regeneration is possible, to alleviate compression of her artery, and to offer relief of her pain and numbness. Of these, the most urgent was to prevent further loss of nerve function by relieving the nerve compression.

TAKE-HOME MESSAGE

Conventional roentgenography, linear tomography, computerized tomography (CT), and MRI are radiographic modalities used to image the thorax, shoulder girdle, and soft tissues. Vascular structures, surface anatomy, and the soft tissues are incompletely imaged by conventional radiographic techniques.

MRI separates proton densities within organ systems and does not require reconstruction or repositioning of the patient. The multiplanar MRI displays the anatomy of the brachial plexus and peripheral nerves for investigation by sequential imaging of landmark anatomy according to proton density distribution.⁷⁻⁹

In our patient, multiplanar imaging allowed definitive landmark anatomy to surgically remove the omovertebral bone, preventing further nerve damage. She underwent surgery for the removal of the omovertebral bone and left first rib resection that relieved some pain and increased left shoulder motion.

ACKNOWLEDGEMENTS

Thanks to Portia Daniels and Steven Do.

REFERENCES

1. Doita M, Iio H, Mizuno K. Surgical management of Sprengel's deformity in adults. A report of two cases. *Clin Orthop Relat Res.* 2000;371:119-124.
2. Atasoy E. Thoracic outlet compression syndrome. *Orthop Clin N Am.* 1996;27:265-303.
3. Lord JW, Rosati LM. Thoracic outlet syndromes. *Clinical Symposia Ciba Geigy.* 1971:1-32.
4. Sunderland S. Blood supply of the nerves to the upper limb in man. *Arch Neurol Psych.* 1945;53:91-115.
5. Collins JD. www.tosinfo.com. Accessed June 2011.
6. Woodburne, RT, Burkel WE. *Essentials of Human Anatomy.* 8th ed. New York, NY: Oxford University Press; 1988:18-216.
7. Clemente, CD. *Anatomy, A Regional Atlas of The Human Body.* 3rd ed. Baltimore, MD: Urban and Schwarzenberg; 1987.
8. Collins JD, Shaver M, Disher A, Miller TQ. Compromising abnormalities of the brachial plexus as displayed by magnetic resonance imaging. *Clin Anat.* 1995;18:1-16.
9. Collins JD. The anatomy of the brachial plexus as displayed by magnetic resonance imaging: technique and application. *J Natl Med Assoc.* 1995;87:489-498. ■